# Hyperpolarised $^{129}$Xe magnetic resonance imaging to monitor treatment response in children with cystic fibrosis

Jonathan H. Rayment[1,2,3], Marcus J. Couch[3,4], Nancy McDonald[1,3], Nikhil Kanhere[3], David Manson[5], Giles Santyr[3,4] and Felix Ratjen[1,2,3]

**Affiliations**: [1]Division of Respiratory Medicine, Dept of Paediatrics, Hospital for Sick Children, Toronto, ON, Canada. [2]Dept of Paediatrics, University of Toronto, Toronto, ON, Canada. [3]Translational Medicine Program, SickKids Research Institute, Toronto, ON, Canada. [4]Dept of Medical Biophysics, University of Toronto, Toronto, ON, Canada. [5]Dept of Diagnostic Imaging, Hospital for Sick Children, Toronto, ON, Canada.

**Correspondence**: Jonathan H. Rayment, Division of Respiratory Medicine, BC Children's Hospital, 4480 Oak Street, Vancouver, BC, Canada, V6H 3N1. E-mail: jonathan.rayment@bcchr.ca

@ERSpublications
**Hyperpolarised $^{129}$Xe MRI is emerging as an important imaging biomarker in cystic fibrosis. Ventilation distribution, measured using this technique, improves after treatment of a pulmonary exacerbation in children with cystic fibrosis.** http://ow.ly/E6Gc30nFMlb

**Cite this article as:** Rayment JH, Couch MJ, McDonald N, *et al*. Hyperpolarised $^{129}$Xe magnetic resonance imaging to monitor treatment response in children with cystic fibrosis. *Eur Respir J* 2019; 53: 1802188 [https://doi.org/10.1183/13993003.02188-2018].

ABSTRACT Pulmonary magnetic resonance imaging using hyperpolarised $^{129}$Xe gas (XeMRI) can quantify ventilation inhomogeneity by measuring the percentage of unventilated lung volume (ventilation defect per cent (VDP)). While previous studies have demonstrated its sensitivity for detecting early cystic fibrosis (CF) lung disease, the utility of XeMRI to monitor response to therapy in CF is unknown. The aim of this study was to assess the ability of XeMRI to capture treatment response in paediatric CF patients undergoing inpatient antibiotic treatment for a pulmonary exacerbation.

15 CF patients aged 8–18 years underwent XeMRI, spirometry, plethysmography and multiple-breath nitrogen washout at the beginning and end of inpatient treatment of a pulmonary exacerbation. VDP was calculated from XeMRI images obtained during a static breath hold using semi-automated k-means clustering and linear binning approaches.

XeMRI was well tolerated. VDP, lung clearance index and the forced expiratory volume in 1 s all improved with treatment; however, response was not uniform in individual patients. Of all outcome measures, VDP showed the largest relative improvement (−42.1%, 95% CI −52.1–−31.9%, p<0.0001).

These data support further investigation of XeMRI as a tool to capture treatment response in CF lung disease.

This article has supplementary material available from erj.ersjournals.com

Received: Nov 16 2018 | Accepted after revision: Feb 02 2019

## Introduction

Overall survival and lung function have improved dramatically over the past decades in patients with cystic fibrosis (CF) [1]. Traditional pulmonary function tests (PFTs) such as spirometry are now often normal in the paediatric age range [2]. As a consequence, the use of spirometric indices as endpoints in clinical trials or for monitoring individual response to therapy, especially in the paediatric population, can be problematic [3]. The lung clearance index (LCI), an outcome measure generated from the multiple-breath washout (MBW) test, reflects ventilation inhomogeneity [4, 5] and has been demonstrated to be more sensitive than spirometry for detecting and monitoring early lung disease in paediatric CF patients [6–8]. Despite its higher sensitivity, MBW testing provides only a whole-lung assessment of ventilation inhomogeneity, and imaging-based measures of lung function may be better at providing insight into the regional nature of disease and detecting subtle, regional pathology.

Hyperpolarised noble gas functional pulmonary magnetic resonance imaging (MRI) has shown considerable advancement over the past decade for the quantification of regional ventilation defects [9], alveolar–capillary gas diffusion [10] and pulmonary microarchitecture [11]. While $^{3}$He was previously the most commonly used inhaled contrast agent in this field, more centres are now using hyperpolarised $^{129}$Xe for functional pulmonary MRI (XeMRI) owing to the lower cost and higher availability of $^{129}$Xe as well as advances in hyperpolarisation physics that have allowed for greater polarisation efficiency of this gas [12]. The most validated hyperpolarised gas MRI technique is static ventilation imaging, which allows for the quantification of ventilation "defects" as a percentage of the total thoracic volume during a breath hold, or ventilation defect per cent (VDP). VDP can be determined using various analytical techniques [9, 13, 14] and has been demonstrated to be more sensitive than spirometry at identifying lung disease in paediatric CF patients [13, 15–17]. In addition, VDP appears to be more sensitive than spirometry and MBW at detecting longitudinal progression of CF lung disease [18]. However, high sensitivity of a test does not necessarily imply responsiveness of that test to treatment. Previous studies using $^{3}$He MRI (HeMRI) outcomes in interventional settings in CF have demonstrated treatment responsiveness of this technique [19–21]. To date, no studies have investigated the ability of XeMRI to assess the efficacy of a therapeutic intervention in the CF population. If this imaging modality is to be used to direct clinical care or as an outcome measure in clinical trials, its ability to detect response to treatment must be further characterised.

In this study, we used a common clinical scenario in CF, in which improvement with treatment is expected, to assess whether XeMRI can detect a treatment response. We performed XeMRI and physiological (spirometry, plethysmography and MBW) testing before and after treatment in children with CF admitted to hospital for treatment of a pulmonary exacerbation. We used this known treatment paradigm to determine 1) whether XeMRI is safe and feasible in a sicker population of paediatric CF patients, 2) if XeMRI can detect changes in regional ventilation distribution following this treatment, and 3) how changes in VDP correlate with changes in spirometric and MBW outcome measures.

## Methods

### *Patient population*

Patients with CF between the ages of 8 and 18 years admitted to hospital for intravenous antibiotic treatment of a physician-diagnosed pulmonary exacerbation were eligible. Exclusion criteria were the inability to perform PFTs or MRI, pregnancy, supplemental oxygen use or a forced expiratory volume in 1 s ($FEV_1$) <40% of predicted at the time of screening. Local ethics board and Health Canada approval was obtained (SickKids REB #1000049033). The study was registered at ClinicalTrials.gov (NCT02606487). The responsible physician determined the treatment regimen. Healthy controls were recruited as part of a separate study (SickKids REB #1000048243, ClinicalTrials.gov NCT02740868).

### *Study protocol*

On the day of testing, inhaled medications were held until testing was complete. Akron pulmonary exacerbation severity (APES) scores were assessed at the time of recruitment [22]. A Likert scale of wellness (1–10) was collected before and after treatment. PFTs, MBW and MRI were performed on the same day within 48 h of the initiation and completion of antibiotic treatment. Spirometry and plethysmography were performed according to American Thoracic Society/European Respiratory Society (ATS/ERS) standards [23, 24]. Nitrogen MBW testing was performed on the Exhalyzer D (Ecomedics, Dürnten, Switzerland) in supine and seated postures, according to standard quality control criteria [5, 25].

Hyperpolarised $^{129}$Xe gas was generated as described (Model 9800; Polarean, Durham, NC, USA) and was dosed at 10% of the participant's total lung capacity (TLC), diluted in ultra high purity nitrogen to a total volume of 1 L for each dose as previously described [26]. XeMRI and conventional proton images were acquired at 3T (Siemens Prisma, Erlangen, Germany) in the coronal plane using a flexible vest radiofrequency coil (for XeMRI images; Clinical MR Solutions, Brookfield, WI, USA) or a flexible torso

array and spine coil (for proton images; Siemens, Erlangen, Germany). The detailed MRI protocol is described in the supplementary material.

### *Image analysis*

Seven slices from each image set (the centre slice plus three flanking slices) were chosen for VDP analysis. XeMRI and proton MRI images were aligned using a semi-automated segmentation approach [26]. VDP was calculated using two approaches: the k-means clustering approach described by KIRBY *et al.* [9] and the mean-anchored, linear binning approach described by COLLIER *et al.* [27]. The VDP threshold in the linear binning technique was estimated from the mean signal intensity distribution of the 10 healthy controls (supplementary material).

### *Statistical analysis*

Statistical analyses were performed using STATA v14 (Stata Corp., College Station, TX, USA). Within-subject absolute changes in outcome measures were post-treatment values minus the pre-treatment values. Within-subject relative changes were the absolute changes divided by the pre-treatment values. Within-subject absolute and relative outcome measure changes are reported with 95% confidence intervals. Correlation of outcome measures was assessed with simple linear regression and the coefficient of determination ($R^2$) is reported.

## Results

### *Patient population*

Between December 2016 and August 2017, 33 children with CF aged between 8 and 18 years admitted to the Hospital for Sick Children for treatment of a pulmonary exacerbation were screened; 20 were enrolled and 15 completed the study (figure 1). Of the enrolled subjects, one could not perform MBW testing, one was unable to correctly complete the breath-hold manoeuvre for XeMRI, and three had their diagnoses of pulmonary exacerbation revised by their treating physicians and were discharged from hospital prior to completing a full course of antibiotic therapy. Data from the 15 participants who completed the study were included in the final analysis and their characteristics are shown in table 1. The median age was 14 years, and baseline lung function was relatively preserved, with a median best $FEV_1$ % pred in the 6 months preceding the pulmonary exacerbation of 85.0% (interquartile range (IQR) 61.0–93.0%).

At the time of admission, the median APES was 11.0 (IQR 8.0–14.0). Mean±SD $FEV_1$ % pred at the time of admission was 62.9±13.9%, which represented a median relative drop of 18.0% (IQR −8.0–−31.0%) from baseline (best $FEV_1$ in the past 6 months). Antibiotic treatment duration was 13 or 14 days for 14 out of 15 participants and 22 days for one participant.

### *XeMRI tolerability and feasibility*

The gas dosing volumes used in this study, as a fraction of TLC, are shown in supplementary table S1. All test procedures were well tolerated. Transient, self-resolving oxygen desaturation (arterial oxygen saturation measured by pulse oximetry ($S_{PO_2}$) of <88% lasting up to 10 s) was observed in 15 out of 30 XeMRI scans (50%). The median oxygen saturation nadir for all scans was 88% (IQR 81–91%). No desaturations lasted

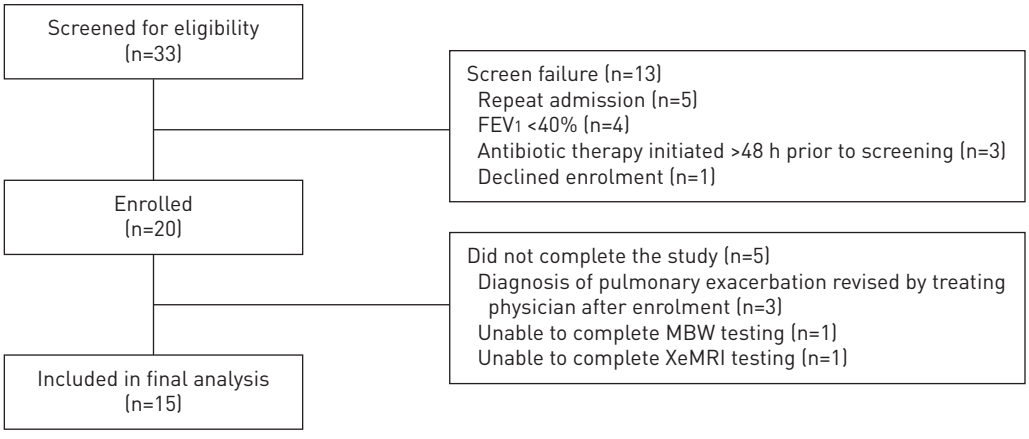


FIGURE 1 Study flow diagram demonstrating screening, enrolment and study completion. $FEV_1$: forced expiratory volume in 1 s; MBW: multiple-breath washout; XeMRI: magnetic resonance imaging using hyperpolarised $^{129}Xe$ gas.

TABLE 1 Baseline and admission characteristics of the participants (n=15)

| Characteristics | |
|---|---|
| **Baseline** | |
| Age years | 14 (13.0–16.5) |
| Male sex | 5 (33.3) |
| Height cm | 153 (148–163) |
| Weight kg | 43.4 (38.2–48.6) |
| Pancreatic insufficient | 12 (80.0) |
| CF liver disease | 1 (6.7) |
| Number of admissions in previous 18 months; mean (range) | 1.2 (0–5) |
| Baseline $FEV_1$ % pred (best in past 6 months) | 85.0 (61.0–93.0) |
| **Admission** | |
| Akron pulmonary exacerbation score | 11.0 (8.0–14.0) |
| Likert wellness score (1–10 scale) | 7 (5–7) |
| Relative drop in $FEV_1$ % pred from baseline on admission | −18.0 (−8.0– −31.0) |
| $FEV_1$ % pred | 62.9±13.9 |
| LCI (sitting) | 15.1±2.4 |
| BMI percentile | 22 (4–39) |
| Positive sputum microbiology at admission | |
| Methicillin-sensitive *Staphylococcus aureus* | 7 (46.7) |
| *Pseudomonas aeruginosa* | 4 (26.7) |
| *Achromobacter* spp. | 3 (20.0) |
| *Aspergillus* spp. | 2 (13.3) |
| *Mycobacterium abscessus* | 2 (13.3) |
| Other | 5 (33.3) |

Data are presented as median (IQR), n (%) or mean±SD, unless otherwise stated. CF: cystic fibrosis; $FEV_1$: forced expiratory volume in 1 s; LCI: lung clearance index; BMI: body mass index.

longer than 10 s and no scans were aborted owing to adverse events. Analysable images were acquired in all but one scanned participant. Representative ventilation defect maps generated using the k-means and linear binning techniques and the corresponding signal histograms are shown in figure 2.

### *Imaging and physiological responses to antibiotic treatment*

Imaging, spirometric, plethysmographic, MBW and symptom score outcomes all improved significantly following treatment (table 2). VDP (calculated using the linear binning technique) showed the greatest mean relative improvement of all outcome measures (−42.1%, 95% CI −57.3–−26.8%, p<0.0001), dropping from a mean of 6.8% to 3.8%. In most participants, the distribution of XeMRI ventilation signal intensity shifted towards the healthy range (the derivation of the healthy distribution can found in supplementary figure S1) but did not completely return to a healthy distribution in any case (supplementary figure S2). Seated LCI showed a significant mean improvement following treatment (−9.1%, 95% CI −15.5–−2.6%, p=0.009), but there was no overall change observed in supine LCI (−2.7%, 95% CI −9.6–4.2%, p=0.4). The distribution of individual relative changes in imaging and physiological outcomes is shown in figure 3. Absolute $FEV_1$ and LCI values correlated with VDP (supplementary table S2). However, there was no correlation between the magnitude of change of the imaging and physiological outcomes.

Unprocessed XeMRI data, signal intensity histograms and physiological data are shown from three cases that exemplify the complementarity of the data obtained using the techniques (figure 4). In patient 20, there was an improvement in $FEV_1$, LCI and VDP (figure 4a). Qualitative analysis of the XeMRI signal histogram generated by the linear binning technique demonstrated resolution of a low-intensity signal plateau seen at the left half of the histogram (figure 4b). In patient 9, treatment resulted in an increase in $FEV_1$, while the LCI and VDP worsened (figure 4c). Qualitative assessment of the XeMRI signal histogram showed a distinct distribution pattern with a very high frequency of lower intensity signal (suggesting widespread regions of poorly ventilated lung) that did not change substantially with treatment (figure 4d). Finally, in patient 13, $FEV_1$ did not improve following treatment, but both VDP and LCI decreased (figure 4e), and the post-treatment XeMRI signal intensity histogram shifted towards the normal range with reductions in focal defects on the XeMRI images (figure 4f).

## Discussion

In this study, we assessed the ability of pulmonary XeMRI to detect changes in ventilation distribution following inpatient treatment of a CF pulmonary exacerbation. The study procedure was well tolerated in

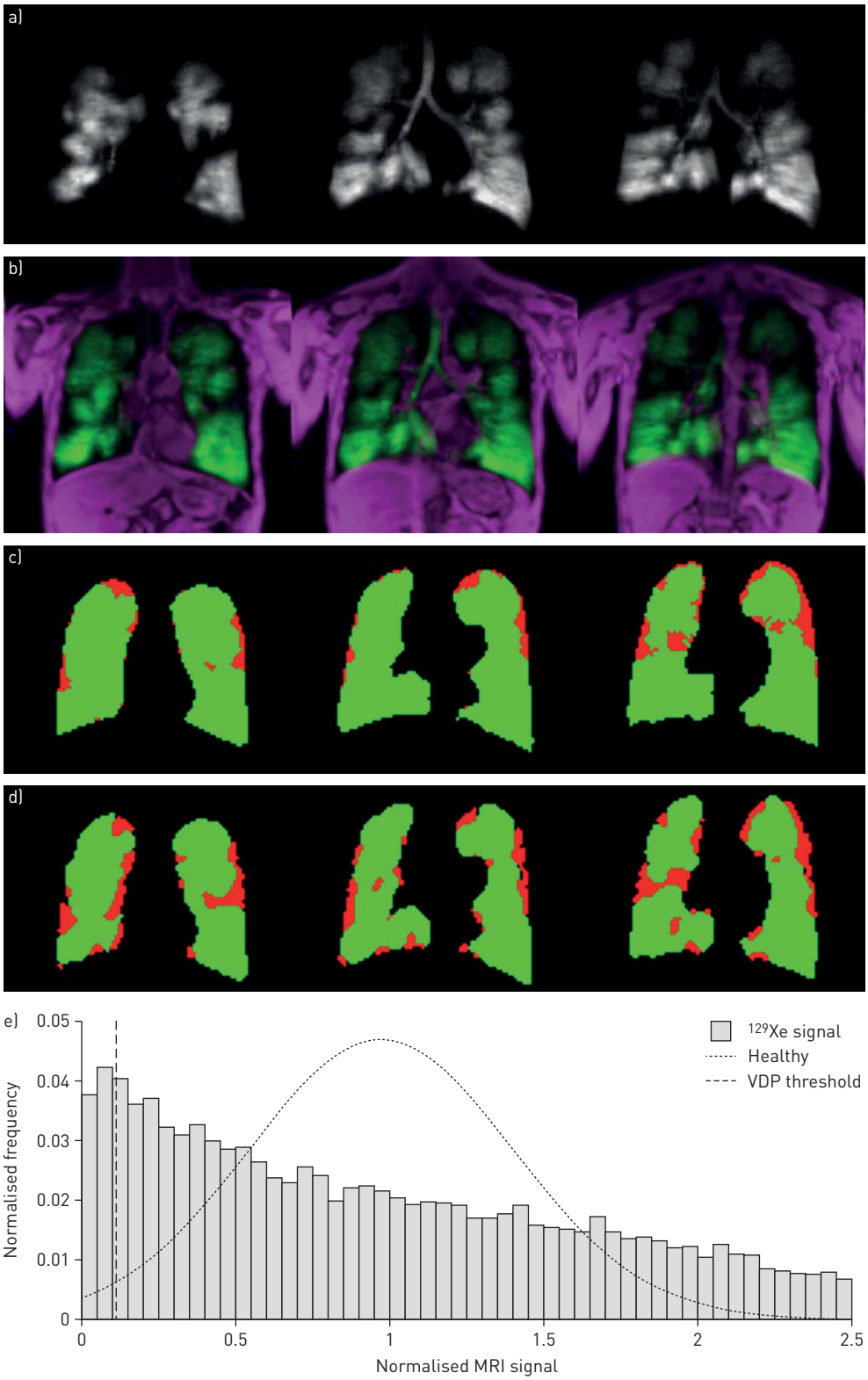


FIGURE 2 Examples of images from magnetic resonance imaging (MRI) using hyperpolarised $^{129}$Xe gas (XeMRI), ventilation defect per cent (VDP) mask overlays and a XeMRI signal intensity histogram from the same participant. a) Unprocessed XeMRI signal. b) Colourised proton MRI (purple) and XeMRI (green) acquisitions after registration (*i.e.* alignment). c, d) Ventilation maps calculated using the k-means (c) and linear binning (d) techniques demonstrating ventilated (green) and unventilated (red) lung. e) XeMRI signal intensity histogram plotting the distribution of normalised voxel intensity, with low signal intensity being shown on the left; the mean healthy intensity distribution is overlaid (dashed line) and the calculated VDP threshold is demonstrated by the vertical line.

TABLE 2 Physiological and imaging outcome measures before and after treatment

| | Pre-treatment | Post-treatment | Within-subject absolute change | Within-subject relative change % |
|---|---|---|---|---|
| **XeMRI outcomes %** | | | | |
| VDP (linear binning) | 6.8±3.8 | 3.8±2.7 | −3.0 (−4.9–−1.1)* | −42.1 (−52.2–−31.9)* |
| VDP (k-means) | 10.4±4.5 | 6.7±4.1 | −3.8 (−5.9–−1.7)* | −34.6 (−49.3–−19.9)* |
| **MBW outcomes (seated)** | | | | |
| LCI | 15.2±2.4 | 13.7±2.4 | −1.5 (−2.4–−0.5)* | −9.1 (−15.5–−2.6)* |
| FRC L | 2.3±0.7 | 2.3±0.7 | 0.0 (−0.6–0.6) | −2.8 (−61.1–57.4) |
| CEV L | 35.6±15.3 | 31.6±14.1 | −4.1 (−6.7–−1.5)* | −10.7 (−16.2–−5.2)* |
| $S_{acin}$ $L^{-1}$ | 0.60±0.38 | 0.45±0.24 | −0.16 (−0.32–0.01) | −15.4 (−36.2–5.3) |
| $S_{cond}$ $L^{-1}$ | 0.15±0.07 | 0.15±0.06 | 0.00 (−0.05–0.04) | 13.2 (−13.2–39.6) |
| **MBW outcomes (supine)** | | | | |
| LCI | 15.4±2.5 | 14.9±2.5 | −0.5 (−1.5–0.5) | −2.7 (−9.6–4.2) |
| FRC L | 2.1±0.6 | 2.0±0.6 | −0.2 (−0.8–0.3) | −1.0 (−23.0–30.7) |
| CEV L | 33.1±13.8 | 29.9±14.2 | −3.2 (−5.4–−1.0)* | −10.2 (−16.2–−4.2)* |
| $S_{acin}$ $L^{-1}$ | 0.61±0.45 | 0.44±0.21 | −0.16 (−0.32–0.01) | −15.4 (−36.2–5.3) |
| $S_{cond}$ $L^{-1}$ | 0.18±0.09 | 0.19±0.07 | 0.00 (−0.05–0.04) | 13.2 (−13.2–39.6) |
| **Spirometry and plethysmography outcomes** | | | | |
| $FEV_1$ % pred | 63.0±13.9 | 80.3±14.6 | 17.4 (12.7–22.1)* | 29.8 (21.1–38.5)* |
| RV/TLC | 37.6±9.6 | 30.3±4.6 | −7.8 (−11.6–−4.0)* | −17.9 (−25.2–−10.6)* |
| FRC L | 2.5±0.7 | 2.4±0.6 | −0.1 (−0.2–0.0)* | −4.1 (−9.1–1.0) |
| **Clinical score outcome** | | | | |
| Likert wellness score 1–10, median (IQR) | 7 (5–7) | 9 (7–10) | 2.0 (0.6–3.4)* | 39.1 (14.5–63.7)* |

Data are presented as mean±SD or mean (95% CI), unless otherwise stated. XeMRI: magnetic resonance imaging using hyperpolarised $^{129}Xe$ gas; VDP: ventilation defect per cent; MBW: multiple-breath washout; LCI: lung clearance index; FRC: functional residual capacity; CEV: cumulative expired volume; $S_{acin}$: acinar lung zone ventilation inhomogeneity; $S_{cond}$: conductive lung zone ventilation inhomogeneity; $FEV_1$: forced expiratory volume in 1 s; RV: residual volume; TLC: total lung capacity; IQR: interquartile range. *: p<0.05.

all cases. We demonstrate responsiveness of this outcome measure, reflected by a significant decrease in poorly ventilated lung (quantified by VDP) following treatment. The change in VDP signal was substantial, with a relative improvement of ∼40%, suggesting that this technique can generate outcomes that are robustly responsive to treatment regardless of the image analysis technique that is used. Importantly, the change in VDP did not correlate with changes in MBW or spirometry outcomes, suggesting that these modalities provide complementary information.

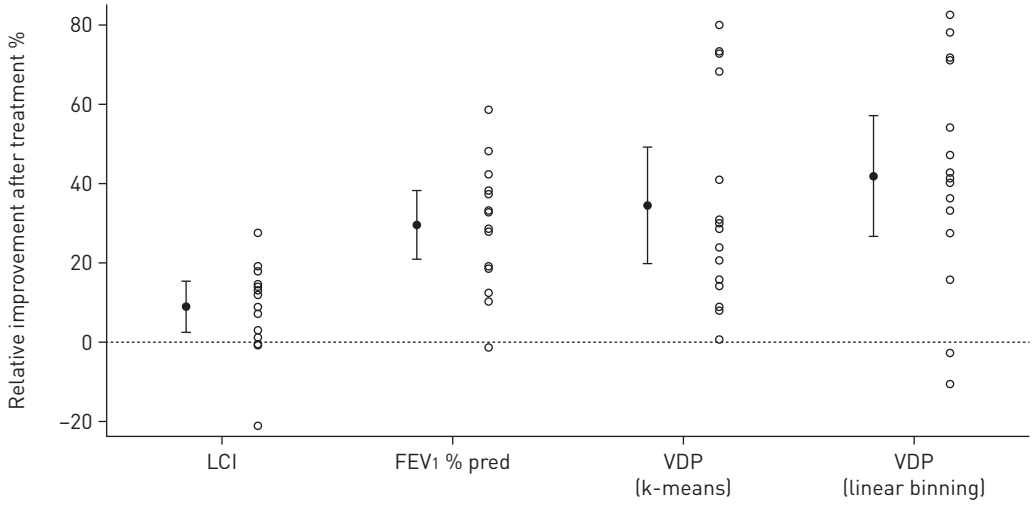


FIGURE 3 Relative improvement of lung clearance index (LCI), forced expiratory volume in 1 s % predicted ($FEV_1$ % pred) and ventilation defect per cent (VDP) (k-means and linear binning techniques) following treatment. Individual relative changes (100% × [pre-treatment value–post-treatment value]/pre-treatment value) are shown by hollow circles. Improvement is always depicted as a positive change regardless of the nature of the outcome measure. The dashed horizontal line indicates "no change". The mean relative change (solid circle) and 95% confidence intervals are shown.

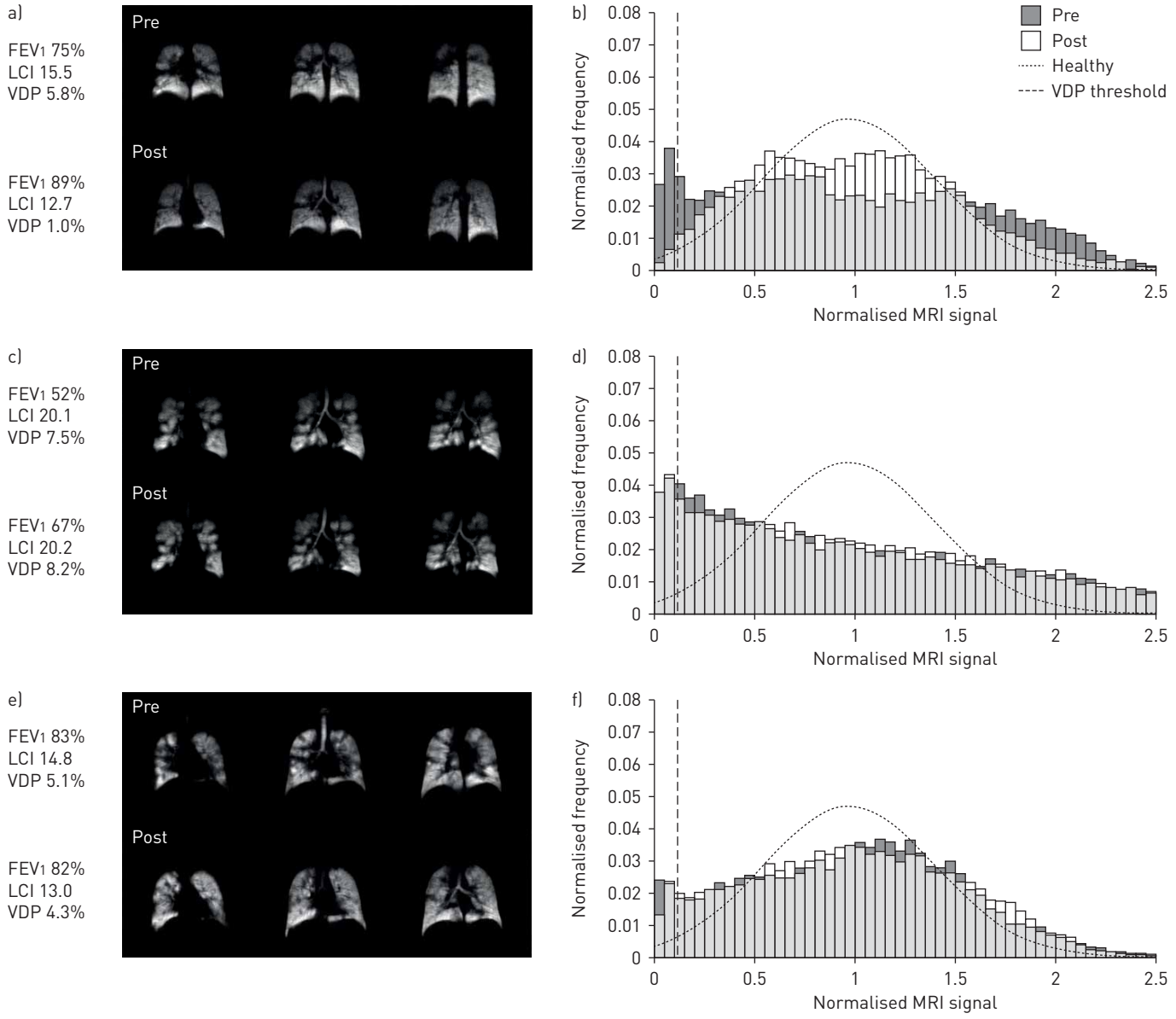


FIGURE 4 Pre- and post-treatment ventilation images from magnetic resonance imaging (MRI) using hyperpolarised $^{129}$Xe gas (XeMRI) (three slices shown) (a, c, e) and signal intensity histograms (b, d, f). a, b) Participant 20; c, d) participant 9; e, f) participant 13. b, d, f) Pre-treatment distribution is shown in dark grey and post-treatment distribution is shown in white; the mean healthy distribution is overlaid with a dashed curve and the calculated ventilation defect per cent (VDP) threshold is identified by a dashed vertical line. FEV1: forced expiratory volume in 1 s; LCI: lung clearance index.

To our knowledge, this is the largest study to investigate hyperpolarised gas functional pulmonary MRI as a tool to monitor treatment response in CF, and the first using XeMRI. One other study has assessed the ability of hyperpolarised HeMRI to detect a treatment response to a pharmacological intervention. In a double-blind study of eight CF patients with gating mutations, Altes *et al.* [19] demonstrated that HeMRI can identify a decrease in ventilation defects after treatment with ivacaftor, a cystic fibrosis transmembrane conductance regulator (CFTR) modulator. Previous HeMRI studies failed to demonstrate a net treatment response to airway clearance therapies using global ventilation defect measures, though the location of the defects changed with treatment [20, 21]. Advanced regional XeMRI image analysis techniques [28] may be able to provide a more detailed physiological quantification of treatment responsiveness; however, data from the ivacaftor study and the current trial suggest that global hyperpolarised gas MRI measures like VDP are responsive to changes in pulmonary ventilation distribution following treatment in CF. More evidence in the interventional setting is needed to define how responsive this technique is to treatment, compared to other available testing modalities.

Another potential clinical role for hyperpolarised gas MRI may be in longitudinal monitoring of CF lung disease. The rate of FEV1 decline in CF is low, even in adulthood [29], and spirometry is typically stably

normal in younger children [30]. Techniques such as MBW are more sensitive than spirometry for detecting the progression of lung disease over time in young children [30], but recent data have suggested that HeMRI (and VDP in particular) may be even more sensitive than MBW for detecting the longitudinal progression of disease [18]. Especially in the era of CFTR modulators, in which we expect the annual rate of lung function decline to be further diminished (or potentially halted) [31], highly sensitive tools to monitor lung function progression over time will become increasingly important to clinical care.

In this study, we confirmed correlations between VDP and both LCI and $FEV_1$ [15, 17]. However, the correlation between VDP and LCI was weaker in the current study than previously observed. This could be because the participants in this study had more severe lung disease, with lower $FEV_1$ and higher LCI than our group's previous assessment of stable CF participants [15]. Additionally these children were also experiencing an acute pulmonary exacerbation. These differences could result in higher variability of measures of ventilation inhomogeneity [32, 33]. Contrastingly, a recent study by Smith *et al.* [17] interrogating regional physiology in children with CF using HeMRI and MBW techniques showed good correlation between VDP and LCI, even in those with worse lung function. However, in this same paper, the authors also demonstrated that as imaged lung volume approached TLC, measured VDP decreased. Measurements in our study were obtained at a lung volume corresponding to ~80% of TLC (supplementary table S1), which is lower than the 60% of TLC that was targeted by Smith *et al.* [17]. It is therefore possible that imaging at a higher lung volume introduced a "ceiling effect" and that VDP was relatively underestimated, especially in smaller patients, thereby decreasing imaging–physiology correlation. This same phenomenon may also have blunted the observed magnitude of treatment response. Gas contrast dosing in future studies should be based on subject lung volumes to minimise this potential confounding effect.

Interestingly, while the absolute physiological and imaging outcome measures were correlated, the magnitude of changes in VDP did not correlate with changes in LCI or $FEV_1$, suggesting that these measures are providing complementary information about treatment response. Examples of individual cases with conflicting results for spirometry, MBW and XeMRI results (figure 4) demonstrate the complementary nature of these tests. Future studies should assess the relationship and combined utility of XeMRI-derived and physiological outcome measures in predicting long-term outcomes and/or disease progression to better define which measurement(s) should be used to best guide treatment decisions.

Somewhat surprisingly, we found that VDP correlated slightly better with seated MBW outcomes (supplementary table S3) than those collected in the supine posture (the posture in which the MRI was performed). This is contrary to recent data that have shown that structural CT scores correlate better with MBW taken in the supine posture [34], though Smith *et al.* [17] also observed slightly better correlation of VDP with seated LCI in their recent paper. The aetiology of this observation is not entirely clear but may again be related to the lung volume at which the XeMRI images were obtained. While the supine posture reduces resting lung volume, performing imaging above the functional residual capacity likely shifts the imaged lung volumes closer to those seen in the sitting position.

One final observation of this study was the impact of disease stability on the postural dependence of MBW outcomes. There is existing evidence that the posture in which MBW testing is performed influences the outcome measures that are generated, with an increase in ventilation heterogeneity seen in the supine posture [35, 36]. We confirmed this finding in the current study, showing that the LCI was significantly higher and the functional residual capacity significantly lower in a supine posture than in a seated posture. This postural dependence of MBW outcomes was diminished (or in the case of LCI, completely abolished) in the pre-treatment participants, but was recovered following therapy (supplementary table S2). These findings are similar to those of Smith *et al.* [35], who found that children with CF had less predictable posture-driven changes in MBW outcomes than those with no lung disease. We hypothesise that mucous plugs, which are a major radiographic feature of CF patients experiencing an exacerbation [37, 38], may shift unpredictably with postural changes, leading to less predictable changes in regional ventilation patterns in sicker patients as they change posture.

Strengths of this study include its prospective design, and the same-day measurement of multiple outcome measures including a standardised approach to the collection and analysis of XeMRI data. The primary limitation of this study is that the intervention studied is not necessarily a scenario in which XeMRI is likely to be used clinically. Similar to what has been done for other outcome measures, pulmonary exacerbations were chosen as a first step of evaluation because of a predictable improvement following treatment in most outcome measures on a group level [39]. Now that XeMRI has been shown to be responsive to treatment in this setting, future studies can assess its responsiveness to other interventions in which smaller signals in traditional PFTs are typically seen [7, 40]. Additionally, structural analysis was not performed in this study. Significant advancements in traditional proton MRI techniques have also been able to demonstrate responses in structural and perfusion scores following therapeutic interventions

in CF, though this responsiveness is variable [37, 41, 42]. The combination of structural and functional MRI techniques will provide important future insights into CF disease mechanisms and treatment responsiveness [43] and should be considered in future studies investigating treatment responsiveness of MRI techniques. Finally, in contrast to current structural MRI techniques [41], the XeMRI performed in this study was limited to participants who were capable of performing an adequate breath-hold manoeuvre. While one study has demonstrated some success in free-breathing infants with HeMRI [44], this remains a significant drawback of this technique.

In conclusion, this study has shown that that XeMRI is responsive to treatment of pulmonary exacerbations in paediatric CF participants, with robust decreases observed in VDP. This demonstrates that XeMRI shows promise as an emerging imaging biomarker for monitoring treatment response in CF. In addition, XeMRI has a potential role as a research tool to better understand the complex and spatially heterogeneous pathophysiology of CF lung disease.

Author contributions: All authors have contributed significantly to the work, have participated in drafting or critically revising the manuscript, have seen and approved the final version of the manuscript, and take responsibility for the content of the manuscript.

Conflict of interest: J.H. Rayment has nothing to disclose. M.J. Couch reports partial salary support from Siemens Healthcare through the MITACS Elevate postdoctoral fellowship programme, during the conduct of the study. N. McDonald has nothing to disclose. N. Kanhere has nothing to disclose. D. Manson has nothing to disclose. G. Santyr has nothing to disclose. F. Ratjen has nothing to disclose.

Support statement: This study was funded by The Irwin Fund and a Canadian Institutes for Health Research Project grant #376120. J.H. Rayment was funded by a Cystic Fibrosis Canada clinical fellowship and M.J. Couch was supported by a MITACS Elevate award. Funding information for this article has been deposited with the Crossref Funder Registry.

## References

1 Stephenson AL, Sykes J, Stanojevic S, *et al.* Survival comparison of patients with cystic fibrosis in Canada and the United States: a population-based cohort study. *Ann Intern Med* 2017; 166: 537–546.
2 Marshall B, Faro A, Elbert A, *et al.* Cystic Fibrosis Foundation Patient Registry 2016 annual data report. Bethesda, Cystic Fibrosis Foundation, 2017.
3 Stanojevic S, Ratjen F. Physiologic endpoints for clinical studies for cystic fibrosis. *J Cyst Fibros* 2016; 15: 416–423.
4 Robinson PD, Goldman MD, Gustafsson PM. Inert gas washout: theoretical background and clinical utility in respiratory disease. *Respiration* 2009; 78: 339–355.
5 Robinson PD, Latzin P, Verbanck S, *et al.* Consensus statement for inert gas washout measurement using multiple- and single-breath tests. *Eur Respir J* 2013; 41: 507–522.
6 Aurora P, Bush A, Gustafsson P, *et al.* Multiple-breath washout as a marker of lung disease in preschool children with cystic fibrosis. *Am J Respir Crit Care Med* 2005; 171: 249–256.
7 Ratjen F, Hug C, Marigowda G, *et al.* Efficacy and safety of lumacaftor and ivacaftor in patients aged 6–11 years with cystic fibrosis homozygous for F508del-CFTR: a randomised, placebo-controlled phase 3 trial. *Lancet Respir Med* 2017; 5: 557–567.
8 Rayment JH, Stanojevic S, Davis SD, *et al.* Lung clearance index to monitor treatment response in pulmonary exacerbations in preschool children with cystic fibrosis. *Thorax* 2018; 73: 451–458.
9 Kirby M, Svenningsen S, Ahmed H, *et al.* Quantitative evaluation of hyperpolarized helium-3 magnetic resonance imaging of lung function variability in cystic fibrosis. *Acad Radiol* 2011; 18: 1006–1013.
10 Driehuys B, Cofer GP, Pollaro J, *et al.* Imaging alveolar-capillary gas transfer using hyperpolarized $^{129}$Xe MRI. *Proc Natl Acad Sci USA* 2006; 103: 18278–18283.
11 Saam BT, Yablonskiy DA, Kodibagkar VD, *et al.* MR imaging of diffusion of $^{3}$He gas in healthy and diseased lungs. *Magn Reson Med* 2000; 44: 174–179.
12 Mugler JP, Altes TA. Hyperpolarized $^{129}$Xe MRI of the human lung. *J Magn Reson Imaging* 2013; 37: 313–331.
13 Thomen RP, Walkup LL, Roach DJ, *et al.* Hyperpolarized $^{129}$Xe for investigation of mild cystic fibrosis lung disease in pediatric patients. *J Cyst Fibros* 2017; 16: 275–282.
14 He M, Driehuys B, Que LG, *et al.* Using hyperpolarized $^{129}$Xe MRI to quantify the pulmonary ventilation distribution. *Acad Radiol* 2016; 23: 1521–1531.
15 Kanhere N, Couch MJ, Kowalik K, *et al.* Correlation of lung clearance index with hyperpolarized $^{129}$Xe magnetic resonance imaging in pediatric subjects with cystic fibrosis. *Am J Respir Crit Care Med* 2017; 196: 1073–1075.
16 Marshall H, Horsley A, Taylor CJ, *et al.* Detection of early subclinical lung disease in children with cystic fibrosis by lung ventilation imaging with hyperpolarised gas MRI. *Thorax* 2017; 72: 760–762.
17 Smith LJ, Collier GJ, Marshall H, *et al.* Patterns of regional lung physiology in cystic fibrosis using ventilation magnetic resonance imaging and multiple-breath washout. *Eur Respir J* 2018; 52: 1800821.
18 Smith L, Marshall H, Aldag I, *et al.* Longitudinal assessment of children with mild cystic fibrosis using hyperpolarized gas lung magnetic resonance imaging and lung clearance index. *Am J Respir Crit Care Med* 2018; 197: 397–400.
19 Altes TA, Johnson M, Fidler M, *et al.* Use of hyperpolarized helium-3 MRI to assess response to ivacaftor treatment in patients with cystic fibrosis. *J Cyst Fibros* 2017; 16: 267–274.
20 Bannier E, Cieslar K, Mosbah K, *et al.* Hyperpolarized $^{3}$He MR for sensitive imaging of ventilation function and treatment efficiency in young cystic fibrosis patients with normal lung function. *Radiology* 2010; 255: 225–232.
21 Mentore K, Froh DK, de Lange EE, *et al.* Hyperpolarized HHe 3 MRI of the lung in cystic fibrosis: assessment at baseline and after bronchodilator and airway clearance treatment. *Acad Radiol* 2005; 12: 1423–1429.

22 Kraynack NC, McBride JT. Improving care at cystic fibrosis centers through quality improvement. *Semin Respir Crit Care Med* 2009; 30: 547–558.
23 Miller MR, Hankinson J, Brusasco V, *et al.* Standardisation of spirometry. *Eur Respir J* 2005; 26: 319–338.
24 Wanger J, Clausen JL, Coates A, *et al.* Standardisation of the measurement of lung volumes. *Eur Respir J* 2005; 26: 511–522.
25 Jensen R, Stanojevic S, Klingel M, *et al.* A systematic approach to multiple breath nitrogen washout test quality. *PLoS One* 2016; 11: e0157523.
26 Santyr G, Kanhere N, Morgado F, *et al.* Hyperpolarized gas magnetic resonance imaging of pediatric cystic fibrosis lung disease. *Acad Radiol* 2019; 26: 344–354.
27 Collier GJ, Acunzo L, Smith LJ, *et al.* Linear binning maps for image analysis of pulmonary ventilation with hyperpolarized gas MRI: transferability and clinical applications. Joint Annual Meeting ISMRM–ESMRMB, 2018. Abstract 4482. Available from: http://archive.ismrm.org/2018/4482.html
28 Horn FC, Marshall H, Collier GJ, *et al.* Regional ventilation changes in the lung: treatment response mapping by using hyperpolarized gas MR imaging as a quantitative biomarker. *Radiology* 2017; 284: 854–861.
29 Stephenson A, Mak D, Mahmood A, *et al.* The Canadian Cystic Fibrosis Registry 2016 annual data report. Toronto, Cystic Fibrosis Canada, 2017.
30 Stanojevic S, Davis SD, Retsch-Bogart G, *et al.* Progression of lung disease in preschool patients with cystic fibrosis. *Am J Respir Crit Care Med* 2017; 195: 1216–1225.
31 Schechter MS, Regelmann WE, Sawicki GS, *et al.* Antibiotic treatment of signs and symptoms of pulmonary exacerbations: a comparison by care site. *Pediatr Pulmonol* 2015; 50: 431–440.
32 Oude Engberink E, Ratjen F, Davis SD, *et al.* Inter-test reproducibility of the lung clearance index measured by multiple breath washout. *Eur Respir J* 2017; 50: 1700433.
33 Svedberg M, Gustafsson PM, Robinson PD, *et al.* Variability of lung clearance index in clinically stable cystic fibrosis lung disease in school age children. *J Cyst Fibros* 2018; 17: 236–241.
34 Ramsey KA, Rosenow T, Turkovic L, *et al.* Lung clearance index and structural lung disease on computed tomography in early cystic fibrosis. *Am J Respir Crit Care Med* 2016; 193: 60–67.
35 Smith LJ, Macleod KA, Collier GJ, *et al.* Supine posture changes lung volumes and increases ventilation heterogeneity in cystic fibrosis. *PLoS One* 2017; 12: e0188275.
36 Prisk GK, Elliott AR, Guy HJ, *et al.* Multiple-breath washin of helium and sulfur hexafluoride in sustained microgravity. *J Appl Physiol* 1998; 84: 244–252.
37 Stahl M, Wielputz MO, Graeber SY, *et al.* Comparison of lung clearance index and magnetic resonance imaging for assessment of lung disease in children with cystic fibrosis. *Am J Respir Crit Care Med* 2017; 195: 349–359.
38 Davis SD, Fordham LA, Brody AS, *et al.* Computed tomography reflects lower airway inflammation and tracks changes in early cystic fibrosis. *Am J Respir Crit Care Med* 2007; 175: 943–950.
39 Horsley AR, Davies JC, Gray RD, *et al.* Changes in physiological, functional and structural markers of cystic fibrosis lung disease with treatment of a pulmonary exacerbation. *Thorax* 2013; 68: 532–539.
40 Milla CE, Ratjen F, Marigowda G, *et al.* Lumacaftor/ivacaftor in patients aged 6–11 years with cystic fibrosis and homozygous for F508del-CFTR. *Am J Respir Crit Care Med* 2017; 195: 912–920.
41 Stahl M, Wielpütz MO, Ricklefs I, *et al.* Preventive inhalation of hypertonic saline in infants with cystic fibrosis (PRESIS): a randomized, double-blind, controlled study. *Am J Respir Crit Care Med* 2018; in press [https://doi.org/10.1164/rccm.201807-1203OC].
42 Wielputz MO, Puderbach M, Kopp-Schneider A, *et al.* Magnetic resonance imaging detects changes in structure and perfusion, and response to therapy in early cystic fibrosis lung disease. *Am J Respir Crit Care Med* 2014; 189: 956–965.
43 Thomen R, Walkup L, Roach D, *et al.* Investigation of structure-function relationships in cystic fibrosis lung disease using hyperpolarized xenon and ultra-short echo MRI. *Am J Respir Crit Care Med* 2018; 197: A6386.
44 Altes TA, Meyer CH, Mata JF, *et al.* Hyperpolarized helium-3 magnetic resonance lung imaging of non-sedated infants and young children: a proof-of-concept study. *Clin Imaging* 2017; 45: 105–110.